Feasibility of Extracting Velocity Distribution in Choriocapillaris in Human Eyes from ICG Dye Angiograms

L. Zhu[1]
e-mail: zliang@umbc.edu

Y. Zheng

C. H. von Kerczek

L. D. T. Topoleski

Department of Mechanical Engineering,
University of Maryland, Baltimore County,
Baltimore, MD 21250

R. W. Flower
Department of Ophthalmology,
University of Maryland at Baltimore,
Baltimore, MD 21250 and
New York University,
New York, NY

Indocyanine green (ICG) dye angiography has been used by ophthalmologists for routine examination of the choroidal vasculature in human eyes for more than 20 years*. In this study, a new approach is developed to extract information from ICG dye angiograms about blood velocity distribution in the choriocapillaris and its feeding blood vessels. ICG dye fluorescence intensity rise and decay curves are constructed for each pixel location in each image of the choriocapillaris in an ICG angiogram. It is shown that at each instant of time the magnitude of the local instantaneous dye velocity in the choriocapillaris is proportional to both the slope of the ICG dye fluorescence intensity curve and the dye concentration. This approach leads to determination of the absolute value of blood velocity in the choriocapillaris, assuming an appropriate scaling, or conversion factor can be determined. It also enables comparison of velocities in different regions of the choriocapillaris, since the conversion factor is independent of the vessel location. The computer algorithm developed in this study can be used in clinical applications for diagnostic purposes and for assessment of the efficacy of laser therapy in human eyes.* [DOI: 10.1115/1.2165692]

Keywords: ICG dye angiography, AMD, blood flow, choriocapillaris

Introduction

The choriocapillaris lies immediately beneath the sensory retina and is separated from it only by Bruch's membrane and the monocellular layer of retinal pigment epithelium (RPE). It provides nutrition to approximately the outer third of the retina via molecular diffusion, except in the thin retinal foveal region, where the choriocapillaris provides nutrition through the entire thickness. A precise description of the human choroidal circulation parameters, such as blood velocity distribution, is fundamental to understanding the choroid's role in the pathophysiology of ocular diseases. In current clinical studies, intravenously-injected indocyanine green (ICG) dye is widely used to study the vasculature in choroid. The ICG dye can reach the large diameter choroidal vessels, the choriocapillaris, choroidal neovascularization (CNV) lesions (when present), and the retinal vessels at different times. The near-infrared wavelengths of ICG dye fluorescence can penetrate the retinal pigment epithelium (RPE) and choroidal pigments, thus enabling the visualization and identification of CNVs and their choroidal feeder vessels with diameters as small as 50 μm. In this study, we aimed to improve and extend the information that can be extracted from indocyanine green dye angiograms by developing a method to determine blood velocity distribution in the choriocapillaris based on the constructed ICG dye fluorescence intensity curves.

The choroid is the posterior segment of the uveal tract, bounded internally by Bruch's membrane and externally by the sclera. At the center of the posterior retina (about 4 mm lateral to the optic disk) is the fovea, which is responsible for the finest visual acuity of the eye and for color vision. Since the fovea is devoid of retinal vessels, the choroid supplies nutrients to the entire foveal thickness and to approximately the outer one third of the rest of the sensory retina thickness via molecular diffusion. The human choroid and its relationship to the sensory retina are shown in Fig. 1.

The choroid has a complicated three-dimensional structure. A top view (from the retinal side) of a corrosion cast of the choriocapillaris has a meshlike appearance (Figs. 1(*d*) and 1(*e*)); the holes (dark areas) bounded by the choriocapillaries are occupied by choroidal tissue. The circulation of blood in the choriocapillaris is similar to blood flow passing an array of tissue columns confined between two flat sheets. The blood supply to the choriocapillaris comes from the underlying choroidal arteries which run, more or less, obliquely to the choriocapillaris (Fig. 1(*e*)). Blood is then collected by the underlying choroidal veins, which also run obliquely or vertically from the choriocapillaris.

Due to the three-dimensional structure of the choroidal vasculature and presence of the overlying retinal circulation, it is difficult to delineate individual choroidal vessels and the choriocapillaries in ICG angiogram images, and to describe quantitatively blood flow parameters, such as velocity, local blood perfusion rate, etc. ICG dye angiography has become a clinical tool [1–5] for the routine diagnosis and management of some diseases, such as choroidal neovascularization (CNV) associated with age-related macular degeneration (AMD). Ninety eight percent of injected ICG dye binds to plasma proteins [6], causing it to remain in the choroidal blood vessel and thus produces a relatively sharp picture of the vessels. After venous injection, a fundus camera is used to record 512×480 pixel images of the eye at a rate of 30 per s; each image pixel corresponds to approximately 13 μm in length [7]. Once the ICG dye appears in a particular vascular compartment, such as the choroidal arterioles, the fluorescence emission of the dye is detected by a CCD video sensor in the fundus camera. Obviously, the more dye in the vessels of the vascular compartment, the brighter the image recorded. The brightness at each image pixel is expressed as a gray scale value, ranging from 0 to 256.

Figures 2(*a*) and 2(*b*) are two ICG dye images of the fundus recorded 2 s apart. Figure 2(*a*) clearly shows the ICG dye filling

[1]Corresponding author.

Contributed by the Bioengineering Division of ASME for publication in the JOURNAL OF BIOMECHANICAL ENGINEERING. Manuscript received August 2, 2004; final manuscript received October 20, 2005. Review conducted by Elaine P. Scott.

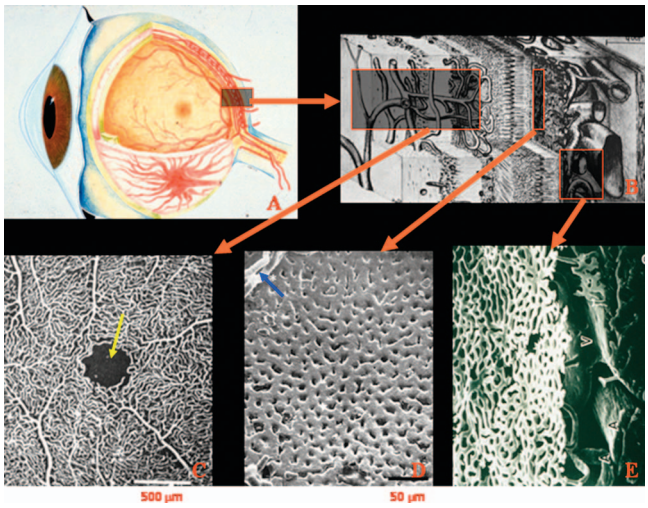

Fig. 1 Anatomic structure of the human eye and its retinal and choroidal vasculatures: (*A*) The eye in cross-section; (*B*) Magnified view of the retinal and choroidal vasculatures. Note that the retinal capillaries permeate the sensory retinal tissue, except for the foveal region, as shown in (*C*); (*C*) Anterior view of the retinal vasculature (corrosion cast), centered on the foveal region (yellow arrow) which is devoid of vessels and capillaries: (*D*) Anterior view of the sub-foveal choriocapillaris (corrosion cast). Note the retinal capillaries (blue arrow) at the edge of the fovea, visible in the upper left-hand corner; (*E*) Oblique sectional view of a corrosion cast of the choroidal vasculature showing the relationship of the choriocapillaris to the underlying choroidal arteries and veins that feed and drain it.

the choroidal arteries underlying the choriocapillaris. Filling of the choriocapillaris occurs later, as shown by Fig. 2(*b*). Thus, this angiographic technique allows visualization of the large choroidal vessels. However, it is difficult to delineate smaller vessels that comprise the complicated meshlike structure of the choriocapillaris. The gray scale values of the pixels in each image indicate only whether blood is present at a specific location; quantitative blood flow parameters, such as velocity and local blood perfusion rate in the choroid and choriocapillaris, are not directly apparent.

Several approaches have been proposed to quantify the choriocapillaris blood circulation, but these are descriptive and lack a rigorous theoretical basis. Most previous studies of choriocapillaris blood flow used "filling time" as a quantitative measure of the blood flow [8,9]. Choriocapillaris "filling time" is defined as

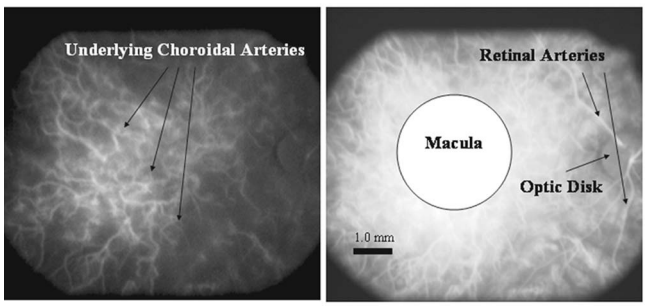

(a) (b)

Fig. 2 Two ICG dye angiogram images taken two seconds apart in a healthy subject. (*a*) ICG dye fills the choroidal arteries underlying the choriocapillaris, and in the macular region filling of the choriocapillaris appears as a faint superficial diffuse fluorescence. Note the clear image of individual choroidal arteries; (*b*) dye now fills the entire choriocapillaris and the choroidal veins and retinal arteries.

the time interval from first appearance of dye in the choriocapillaris to first appearance of dye in the choroidal venules. Use of this definition usually involves subjective interpretation. In some studies, filling time has been defined to be the time interval from dye injection to the achievement of 10% or 63% of the maximum ICG fluorescence intensity achieved during dye bolus transit [10,11]. Analyses of clinical ICG dye angiograms by several investigators have demonstrated that choriocapillaris blood flow in AMD-affected eyes is significantly slower than in normal eyes [8,9,11,12]. In two studies, high-speed ICG fluorescence angiograms were analyzed by subtracting of sequential images, producing images in which the gray scale value is proportional to the slope of the ICG dye intensity versus time curve [8,13]. This method has been used to describe the filling speed of the choriocapillaris [11]. Although this approach seems reasonable, the effects of the vascular geometry and light absorption by the various layers of tissue in the fundus of the eye were not assessed in these studies. From a qualitative point of view, a shorter filling time, or a steeper slope of the time-varying ICG dye intensity curve, should be associated with a faster blood flow in the choriocapillaris. However, it is not clear from previous studies whether or not a single calibration factor can be used to convert the filling time, or slope, to blood flow velocity in comparing velocities from one region of the choriocapillaris to another. Due to spatially varying vascular architecture and attenuation of the ICG dye fluorescence emission, it is likely that neither the filling time nor slope, alone, is adequate to provide the necessary conversion to blood velocity. It would be extremely useful, therefore, to use the information contained in high-speed ICG dye angiograms to determine quantitative point-to-point blood velocity distribution throughout the choriocapillaris.

Methods and Algorithm Formulation

ICG Dye Angiogram Images. Images from high-speed (30 images/s) ICG dye fluorescence angiography performed on healthy subjects were used in this study. The field of view in each angiogram was 30 deg, the spatial resolution of each image was 512×480 pixels, and brightness was recorded on a 256 level gray scale. Angiography was performed by intravenous injection of 0.3 ml of 25 mg/ml ICG dye in an aqueous solvent, followed by rapid injection of a 5 ml normal saline flush. This injection regimen results in a peak dye concentration of around 0.03 mg/ml in the intraocular vessels which results in the maximum ICG dye fluorescence in blood. In an angiographic image, the gray scale brightness of each pixel is referred to as the instantaneous dye fluorescence intensity, I, since fluorescence intensity is a function of the total amount of dye present. By aligning the sequential images, the time-varying ICG dye fluorescence intensity for each location (pixel) in the field of view of the fundus of the eye could be described. For a given pixel, the intensity was plotted as a function of time to generate the dye intensity curve.

Analysis. Consider a straight and rigid blood vessel through which a dye bolus is passing at the speed U_∞, as shown in Fig. 3. It is assumed that the concentration of the dye bolus varies along its streamline (the axis of the blood vessel) and that the concentration is independent of the vascular cross-sectional area normal to the flow direction. Fluorescent light emitted from the dye passes through the vessel surface and is eventually received by the camera. The small square in the illustration represents one image pixel, having width dp. The total emission, $I(t)$, received by the camera from each pixel location at a given instant in time is assumed to be proportional to the amount of dye [14] in the blood volume beneath the pixel and is given by

$$I(t) = EC(z)A_{\text{area}}dp = EC(U_\infty t)A_{\text{area}}dp \tag{1}$$

where $C(z)$ is the dye concentration of that location at time t, E is a constant accounting for the absorption of fluorescent light by the tissue between the vessel wall and the camera, U_∞ is the blood

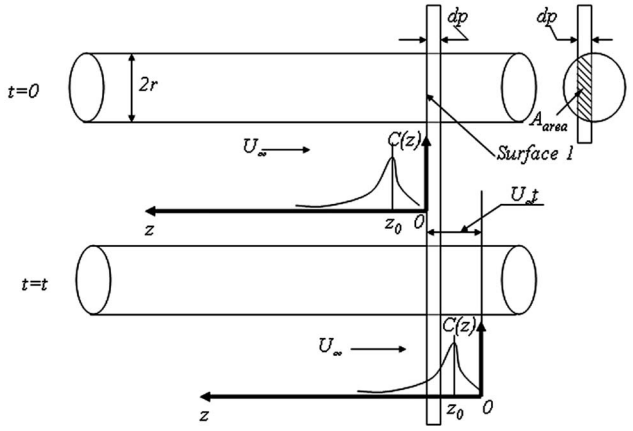

Fig. 3 Schematic diagram of a dye bolus traveling along a straight blood vessel segment. The dye bolus may have an arbitrary concentration distribution in the axial direction, $C(z)$. dp denotes the dimension of each image pixel, and A_{area} represents the cross-sectional area of the volume contributing to the dye intensity in that pixel location.

flow velocity, dp is the width of the pixel, and A_{area} is the cross-sectional area of the blood volume, as shown by the shadowed area in Fig. 3. Note that the dye fluorescence intensity, I, should reach its maximum when the maximum concentration of the dye passes the pixel.

Figure 4 shows a time-varying dye fluorescence intensity curve for one pixel, which can be constructed from ICG dye angiograms. According to Eq. (1), the dye fluorescence intensity curve ($I(t)$) is a scaled mirror image of the dye concentration curve ($C(z)$), because of the t to z transformation, as indicated in Fig. 4. The influence of blood flow velocity on the fluorescence intensity curve is to stretch it (in the case of slow flow) or to contract it (in the case of fast flow).

In a one-dimensional system of fluid mechanics, the velocity and other properties of fluid particles are considered to be functions of time and fixed spatial coordinates independent of time. The former is called the Lagrangian description, and the latter the Eulerian description. In the Lagrangian description, the substantial differentiation is described as if the coordinates follow the particles. In the Eulerian description, the differentiation is simply the

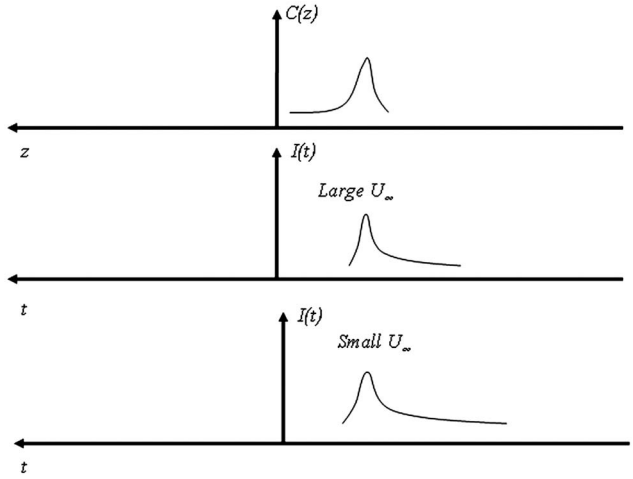

Fig. 4 Dye concentration $C(z)$ and constructed dye intensity $I(t)$ curves

partial derivative of the properties with respect to the coordinates. When the dye intensity is considered in this paper, the relationship between these two derivatives are described by

$$\frac{DI}{Dt} = \frac{\partial I}{\partial t} + U\frac{\partial I}{\partial z} \tag{2}$$

The substantial derivative on the left-hand side of the equation (DI/Dt) represents whether the dye bolus changes its shape with time if we follow the bolus, while the first term on the right-hand side of the equation ($\partial I/\partial t$) denotes how the amount of dye changes by time at fixed spatial coordinates. Previous studies by one of the co-authors [16,17] have quantified the dye concentrations in ocular blood vessels. Their results indicated that there is no significant change in the shape and peak concentration of the dye bolus from upstream vessels (such as choroidal arteriole) to downstream vessels (such as choriocapillaris and choroidal venule). Based on the previous experimental measurements, we assume that the change of the dye bolus shape due to diffusion is negligible along the vessel. Therefore, the substantial differentiation (DI/Dt) is zero. The above equation can then be simplified as

$$0 = \frac{\partial I}{\partial t} + U_\infty\frac{\partial I}{\partial z} \text{ or } \frac{\partial I}{\partial t} = -U_\infty\frac{\partial I}{\partial z} \tag{3}$$

We also assume that E, A_{area}, and dp are constant along the blood vessel, although they may change from vessel to vessel. Substituting the dye concentration expression (Eq. (1)) yields

$$\frac{\partial I}{\partial t} = -EA_{area}dp\frac{\partial C}{\partial z}U_\infty$$

$$U_\infty = \frac{\dfrac{\partial I}{\partial t}}{-EA_{area}dp\dfrac{\partial C(z)}{\partial z}} \tag{4}$$

Note that the blood flow velocity indeed determines how fast the dye intensity rises or decays and the temporal gradient of the dye intensity is directly related to U_∞, as previously indicated [15].

Equation (4) cannot be used directly to calculate the blood flow velocity U_∞, since both E and A_{area} are unknown and they may vary from one blood vessel to another. Rearranging Eq. (1) yields that $EA_{area}dp = I(t)/C(z)$. Substituting for $EA_{area}dp$ in Eq. (4) eliminates both E and A_{area} and then the blood flow velocity, U_∞ can be extracted from the temporal gradient of the dye intensity

$$U_\infty = \left[\frac{\partial I(t)}{\partial t} \Big/ I(t)\right] \Big/ \left[-\frac{\partial C(z)}{\partial z} \Big/ C(z)\right]$$
$$= \left[\frac{\partial I(t)}{\partial t} \Big/ I(t)\right] \Big/ F \tag{5}$$

where F is defined as the conversion factor that depends only on the dye concentration curve $C(z)$. One of the main objectives of this study was to identify a single conversion factor that allows comparison of velocity from one location to another. The ICG dye bolus concentration changes significantly as it circulates from the injection site to the eye. However, once it enters the eye, the peak ICG dye concentration does not change significantly from vessel to vessel, as shown by previous experimental studies [16,17]. In addition, the previous studies suggested very similar shapes of time-varying dye intensity curves for both choroidal arteries and choroidal veins. Therefore, as shown in Eq. (5), so long as the dye bolus retains its profile along the axial direction of the blood vessel, it is reasonable to assume that the denominator in Eq. (5) (i.e., the conversion factor F) is independent of the spatial location and is, therefore, a constant. The denominator can be calibrated by tracing movement of the dye bolus front along a rigid blood vessel, and the calibration will be described later. Then, the absolute value of blood velocity in a single blood vessel can be determined.

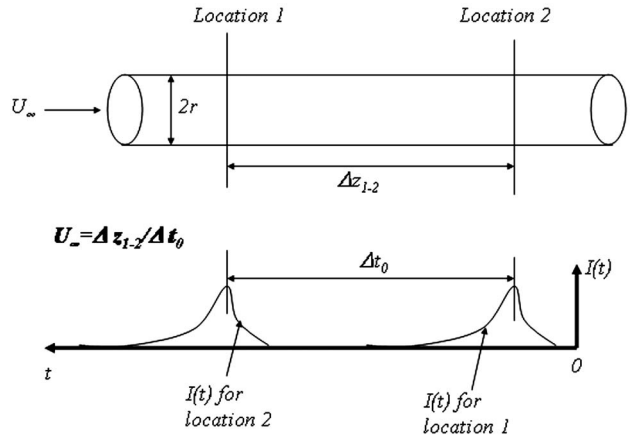

Fig. 5 ICG dye intensity curve at two axial locations along a blood vessel. Δz_{1-2} is the axial distance between locations 1 and 2, and Δt_0 is the time interval between the two peaks in the dye intensity curves.

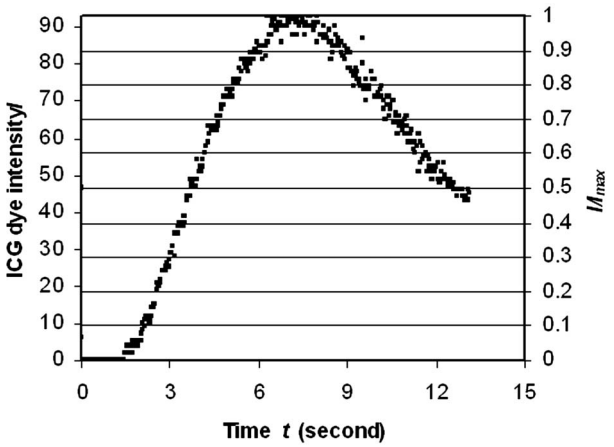

Fig. 6 Constructed ICG dye intensity curve at one spatial location. The left-hand y-axis denotes the ICG dye intensity $I(t)$ or gray value at any time instant, and the right-hand y-axis represents the dimensionless dye intensity $I(t)/I_{max}$.

The numerator in Eq. (5) can be determined by the slope, $\partial I/\partial t$, and the dye fluorescence intensity, I, at any time instant. $\partial I/\partial t$ represents how the dye intensity changes during a time duration, and ideally, it can be calculated by any two sequential measurements of I from the curve. However, we will show later that the data of the intensity curve I are scattered. This causes inaccuracy in the determination of the slope, $\partial I/\partial t$ from two sequential measurements of I and the time duration between them (around 0.013 s). In this study the determination of the numerator in Eq. (5) is performed based on curve fitting of a portion of the intensity curve over several seconds.

Choriocapillaris blood flow can be pulsatile [8], but Eq. (5) still can be used to study the pulsatile behavior of choriocapillaris blood flow. In this study, however, the particular ICG dye angiogram segments used do not possess significant pulsatile behavior, thus the constructed blood flow velocities are essentially constant with time.

Due to the three-dimensional structure of the choroidal vasculature, the ICG dye fluorescence signal recorded in each angiographic image is the combined fluorescence from the multiple overlying vascular layers, including the overlying retinal vessels. However, under normal circumstances, an injected ICG dye bolus wave front reaches the different vasculature layers at different times: choroidal arteries first, then choroidal arterioles, choriocapillaris, choroidal venules and veins, and finally the retinal vasculature. Note that Fig. 2(*b*) clearly shows that the optic disk, the retinal vessels and their branches fill at a later time than the choroidal vessels (Fig. 1(*a*)). Thus, as expected, filling of the retinal vessels in the macular region occurred in later angiogram images than those used in the present study. It is reasonable then to assume that the macular region ICG dye fluorescence intensities analyzed in the present study came entirely from the choriocapillaris and the underlying choroidal vessels.

Calibration of the conversion factor F requires actual measurement of the velocity of blood vessels using other approaches. In this study, we selected individual vessels of uniform size and assumed that the blood flow velocity is constant along the vessel. The intensity curve can be constructed for two different pixel locations along the vessel. As shown in Fig. 5, the intensity curves of those two locations should be similar, except that the peak intensities occur at different times. The spatial distance (Δz_{1-2}) between these two locations can be measured from the angiographic image and the time difference (Δt) can be determined from the two intensity curves. Therefore, the velocity of the blood vessel can be calculated by $V_{1-2}=(\Delta z_{1-2}/(\Delta t)$. After determining the velocity, the numerator in Eq. (5) can be calculated based on one of the intensity curves. The conversion factor is then determined by

$$F = \frac{\dfrac{\partial I(t)}{\partial t} \Big/ I(t)}{V_{1-2}} \tag{6}$$

A Matlab® code was written to implement a computer algorithm that determines the gray scale value (ICG dye fluorescence intensity) at each pixel location of each angiographic image and to plot the intensity versus time curve representing intensity changes throughout an image sequence. The numerator in Eq. (5) was also calculated by the Matlab® code.

Results

Figure 6 is a typical intensity curve constructed for one pixel from a healthy young subject's angiogram. Note that the fluorescence intensity rises quickly to its peak value and remains constant for approximately 2 s. After that it decays, and eventually returns to baseline level. The maximum dye fluorescence intensity (I_{max}) at each pixel location can be identified by the computer algorithm. The data are normalized by calculating the dimensionless ICG dye intensity (I/I_{max}) at this location, represented by the right y-axis in Fig. 6. Considering that the ICG dye enters the underlying choroid arteries first, it is reasonable to speculate that the dye intensity in the first half of the curve is associated with dye in the underlying choroid arteries, while the second half of the curve is associated with dye in the choriocapillaris. But in fact, at some locations fluorescence intensity reaches a first maximum, then very rapidly decreases and then increases to a second maximum, all in significantly less time than required for two heartbeats to occur. The first maximum can be interpreted as the dye reaching its maximum level in the underlying choroidal artery, and the second maximum as the dye reaching its maximum in the choriocapillaris.

In the algorithm developed for this present study, the 20%–40% intensity rise and the 70%–90% intensity rise seen in the time-varying fluorescence curves derived for each pixel location in angiogram images were fitted by exponential functions $D_1e^{t/\tau 1}$ and $D_2e^{t/\tau 2}$, respectively. The constant D and the time constant τ were determined using the least square residual fit. It can be shown that the numerator in Eq. (5) is then equal to $1/\tau$. Thus, the inverse of the fitted time constants, $1/\tau_1$ and $1/\tau_2$ can be used to calculate the average blood flow velocities of the underlying choroidal arteries and the choriocapillaris throughout the risetime portion of

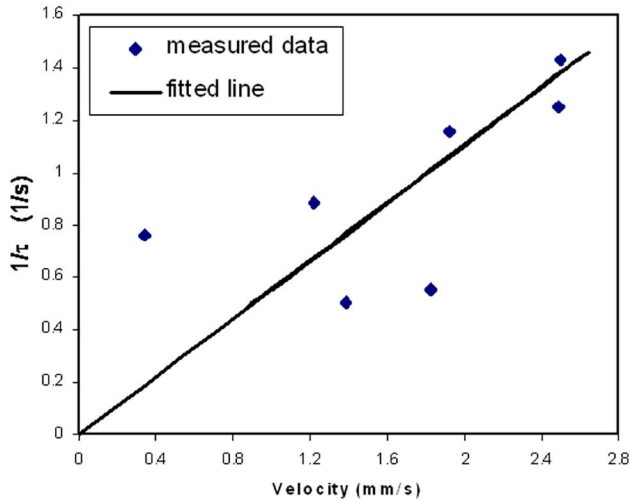

Fig. 7 Relationship between the measured velocity U_∞ and the inverse of the fitted time constant $1/\tau$ in several retina vessels. The solid line is the least square residual fit, and its slope (m^{-1}) is the value of the denominator in Eq. (3). The slope is used as the converting factor for the velocity of the choriocapillaris.

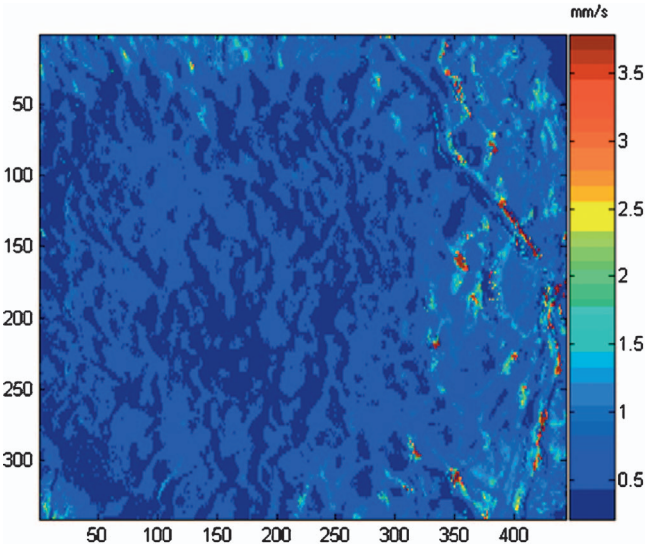

Fig. 9 Two-dimensional mapping of the velocity distribution in the choriocapillaris. The color bar gives the relationship between the color and velocity (mm/s).

the time-varying dye intensity curve at any specific image pixel location. Note that the calibration constant may be different if a different part of the $I(t)$ curve is used for the curve fitting.

In this study, we did not perform the calibration for the underlying choroidal arteries, since these vessels are not parallel to the imaging plane; these arteries traverse the choroidal tissue obliquely from their point of insertion through the wall of the eyeball to enter into the anterior aspect of the choriocapillaris plexus. For the choriocapillaris, the calibration was performed by using the large retinal vessels shown in the right side of the image, as seen in Fig. 2(*b*); these arteries, which fill late in the angiogram, are parallel to the imaging plane. The relationship between the calibrated velocity and $1/\tau$ is shown in Fig. 7. The slope of the straight line in the figure is the best fit of the calibration factors (F) for the choriocapillaris.

The two-dimensional mapping of the $1/\tau$ distribution in the choroidal arteries is shown in Fig. 8. Note that the conversion factor F has not yet been determined. However, it is known that the blood velocity distribution is proportional to $1/\tau$. Different colors in this figure can be used to compare the magnitude of the velocity from one location to another. This approach enables visualization of the large underlying choroidal arteries, wherein the edge of the vessel is represented by an abrupt change of the color. The profile of the $1/\tau$ distribution in the choroidal arteries in Fig. 8 is strikingly similar to that in Fig. 2(*a*) (both are from the same subject). This agreement implies that the computer algorithm developed in this study is a reasonable approach to extracting velocity information. Higher blood flow velocity is observed in the choroidal arteries located in the central region of the retina than in the peripheral region. This implies a larger blood perfusion rate to the choriocapillaris in the macula. Figure 9 shows the velocity distribution in the choriocapillaris, for which conversion factor F was determined based on the data in Fig. 7. For most of the choriocapillaris, the velocity distribution is relatively uniform, approximately 1 mm/s.

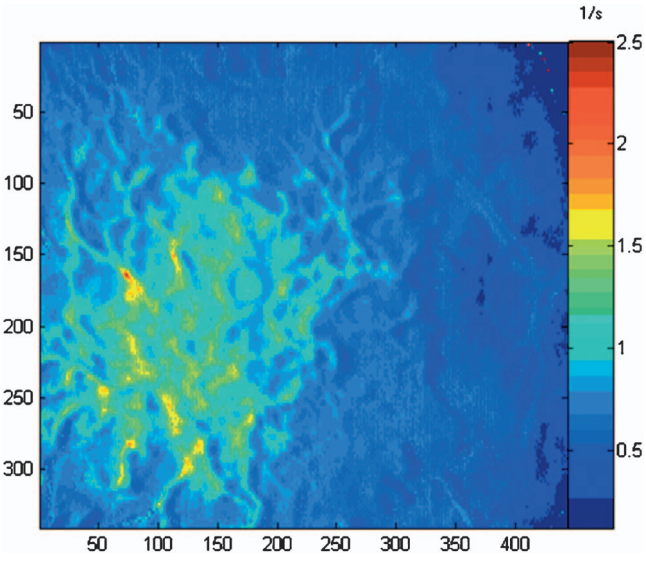

Fig. 8 Velocity distribution in the underlying large choroidal arteries. Note that the velocity has not been calibrated and that the color bar denotes $1/\tau$.

Discussion

It has been difficult to delineate the choriocapillaris, even when using the more advantageous characteristics of ICG dye excitation and emission wavelengths for penetration of fundus pigmented tissues, compared to those of sodium fluorescein dye. Because of the multilayered organization of the choroidal vasculature and the overlying retinal vessels, distinguishing the choriocapillaris is difficult, and extracting the velocity distribution in individual choriocapillaries is complicated. In the present study, for example, the meshlike structure of the choriocapillaris (Fig. 1) is not apparent in the constructed velocity distribution images. In principle, the velocities at the locations of the tissue columns between the individual choriocapillaries should be zero. However, the expected sharp transitions from zero to a finite velocity pattern are not observed in the 2D velocity mapping, since such transitions are below the threshold of the spatial resolution. Considering that the resolution of the pixels forming each angiogram image (13 μm) is comparable to the size of the tissue columns ($\sim$10 μm) and to the size of the choriocapillaries themselves (15–20 μm diam), the image resolution is not high enough to distinguish the tissue columns from the surrounding choriocapillaries.

Nevertheless, in this study we have shown the feasibility of extracting the velocity distribution in the choriocapillaris based on a rigorous mathematical derivation. Our results confirm the corre-

lation between the slope of the dye fluorescence intensity curves and blood flow velocities in the choriocapillaris, as suggested by previous investigators. Further, local velocities not only are proportional to the slopes of the time-varying dye intensity curves for the individual image pixels, but also are inversely proportional to the dye intensity at that time instant. Due to the variations of light absorption by tissue at different locations, large errors may occur when slope alone is used to compare velocities from different locations.

The algorithm developed during the study is only a first step toward quantifying the blood flow parameters in the choroid and choriocapillaris. While our technique addresses many questions related to the descriptive approaches used in clinical assessments of the choroidal circulation, it certainly has limitations. Blood flow velocity data are required for precise calibration of the conversion factor (F, Eq. (5)). To derive the blood flow velocity, two parameters are needed: first, the time interval during which the dye bolus moves from one location to another; and second, the spatial distance between the two locations. To determine the latter parameter from the angiographic image, the blood vessel must be positioned parallel to the image surface. This requirement eliminates many blood vessels for calibration and only a few locations are useful, for example, the choroidal arteries, as pointed out earlier. Therefore, the accuracy of converting $1/\tau$ (the denominator in Eq. (5)) into blood velocity is uncertain. There is only limited information about choriocapillaris blood velocity in the literature. One choriocapillaris blood velocity measurement was around 2.5 mm/s, based on sequential subtraction of high-speed ICG angiogram images [18]; another study [19] that traced the movements of leukocytes in choroidal vessels suggested a velocity variation from 0.48 mm/s (peripheral choriocapillaris) to 2.45 mm/s in the posterior choroid. The reconstructed velocity field in the current study is in this range, thus, lending some credibility to the current analysis.

In conventional ICG dye angiography, the observation of the choriocapillaris and choroid is best accomplished with a spatially concentrated dye bolus having a sharply defined wave front. For example, if the bolus extends significantly along the axial direction of the choroidal arteries, dye fluorescence from the choriocapillaris can be obscured by fluorescence from residual dye simultaneously present in the underlying choroidal arteries. A similar difficulty is encountered when the blood velocity distribution is extracted from the dye fluorescence intensity versus. time curve. An elongated dye bolus necessarily is the direct result of intravenous dye injection, as used in the current clinical applications. It has been demonstrated that directly injecting dye into the carotid artery in the monkey produces a much sharper dye front, and smaller dye bolus have been observed [17]. Unfortunately, it is not practical to apply this technique directly to human subjects. As a consequence, it is extremely difficult to isolate choriocapillaris dye-filling and to separate choriocapillaris blood flow velocity from that of the underlying choroidal arteries. Previous research [8] has suggested that it is possible only if the blood flow velocity of the large choroidal artery is small compared with that in the choriocapillaris.

Other methods available for quantifying blood flow in the retina and choroid include laser Doppler flowmetry and laser speckle flowmetry. The retinal flowmeter based on laser Doppler shift [20] cannot be used to assess the choroidal blood circulation in the same sense as in the present study because the flowmeter cannot distinguish between Doppler shift signals resulting from choriocapillaris blood flow and those resulting from blood flow in the underlying larger choroidal vessels and the overlying retinal vessels. In addition, the output from laser Doppler shift is measured in hertz, and not in easily interpretable units of velocity [21]. Varying optical properties in tissue and lack of a comparable standard and preset controlled conditions make it difficult to convert laser output to velocity in absolute units. Laser speckle flowmetry [22] is based on the correlation between laser speckle fluctuations and the motion of particles in the targeted tissue volume. Its limitations include shallow penetration depth (<1 mm) and difficulty in obtaining the absolute value of the velocity. Similar to laser Doppler flowmetry, both techniques are more suitable for monitoring the temporal response of blood flow to internal and external stimulation [23]. In both of these techniques, it is hard to quantify blood flow variation from one region to another because of the nonhomogeneity of light absorption in tissue. In the current study, it is clear that the ICG dye absorption in tissue can affect the dye intensity recorded by the image (see Eq. (1)). However, the algorithm used in this study has eliminated those effects by introducing a relative value of the gray scale number. As shown in Eq. (5), the final expression depends only on a single conversion factor and does not require the detailed information of the regional variation of the vessel size (A_{area}) and the light absorption in tissue (E).

The technique developed in this study is capable of determining the local choriocapillaris blood flow velocities at each time instant using high-speed ICG angiography. The monotonic behavior of both the rise and decay in time-varying dye fluorescence intensity curves suggests that the blood flow velocity in the choriocapillaris is relatively stable. The good fit of an exponential function to the intensity decay indicates that the velocity is fairly constant. Our derivation shows that the inverse of the time constant is an accurate index to the average blood flow velocity at any location. In an analogous effort to quantify blood circulation in the liver, a previous clinical study in hepatocellular injury patients [24] used the elimination rate constant (equivalent to the inverse of the time constant in this study) to evaluate the hepatic dysfunction. If the elimination rate constant is indeed proportional to the flow velocity, a too-high or too-low elimination rate constant suggests an abnormal blood circulation in the liver. Our approach agrees well with this study.

Two-dimensional mapping of the velocity distribution describes the regional variation of blood flow in the choriocapillaris. Our results have shown a relatively uniform velocity distribution in the macular region of the choriocapillaris. Since the constructed velocity distribution is based on the ICG dye angiograms of only two subjects, we are not sure whether this is true for all healthy subjects or patients with ocular diseases such as AMD. In most AMD patients, the symptom is associated with development of drusen (yellowish deposit) in Bruch's membrane. In recent years, clinical studies [25,26] have shown that vascular change may be induced by various ocular diseases. For AMD patients, the filling time of the choriocapillaris is significantly longer than that in healthy eyes [9,27]. Longer filling time suggests slower blood flow velocity, which may be caused by changes in the pressure gradient and/or flow resistance in the choriocapillaris in AMD patients [28,29]. If the abnormal vascular pattern is indeed a factor contributing to the later formation of drusen in AMD patients, the current computer algorithm can provide a quantitative measure to clinicians for early diagnosis of AMD or other ocular diseases before major symptoms occur.

Quantification of the blood velocity distribution is of clinical importance in laser treatment of AMD and other retina diseases. Most of the laser treatments involve laser photocoagulation of specific blood vessels and usually result in significant changes in the local choriocapillaris blood circulation. Understanding the velocity in the targeted vessel will help clinicians determine the thermal dose during the treatment. In addition, a recent theoretical analysis [30] of velocity fields in the choriocapillaris before and after indirect laser photocoagulation of the feeder vessel for AMD-related choroidal neovascularization suggested that the clinician should select a feeder vessel with large velocity to maximize the treatment efficacy. Therefore, the approach developed in this study will also help provide useful guidance for ophthalmologists to determine favorable factors that lead to successful obliteration of blood vessels. Detailed velocity distribution before and after laser treatment can be used to assess efficacy of the laser therapy.

In conclusion, the feasibility of extracting choriocapillaris blood flow velocity distribution from high-speed ICG fluorescence angiograms was explored, and two-dimensional map of the velocity field were constructed based on a rigorous theoretical derivation. This approach, in spite of its current limitations, is a first step to quantify the blood flow field in the human choriocapillaris. It extends the application of the currently used ICG dye angiography, and it can be used in the future to help clinicians in early diagnosis of ocular diseases and assessment of efficacy of laser therapy.

Acknowledgment

This research was supported by a UMBC Summer Faculty Fellowship to Liang Zhu.

References

[1] Asrani, S. S., D'Anna, Z. S., Phelan, A., Goldberg, M., and Zeimer, R., 1996, "Selective Visualization of Choroidal Neovascular Membranes," Invest. Ophthalmol. Visual Sci., **37**, pp. 1642–1650.

[2] Kramer, M., Mimouni, K., Priel, E., Yassur, Y., and Weinberger, D., 2000, "Comparison of Fluorescein Angiography and Indocyanine Green Angiography for Imaging of Choroidal Neovascularization in Hemorrhagic Age-Related Macular Degeneration," Am. J. Ophthalmol., **129**, pp. 495–500.

[3] Pauleikhoff, D., Spital, G., Radermacher, M., Brumm, G. A., Lommatzsch, A., and Bird, A. C., 1999, "A Fluorescein and Indocyanine Green Angiographic Study of Choriocapillaris in Age-Related Macular Disease," Arch. Ophthalmol. (Chicago), **117**, pp. 1353–1358.

[4] Reichel, E., Puliafito, C. A., Duker, J. S., and Guyer, D. R., 1994, "Indocyanine Green Dye-Enhanced Diode Laser Photocoagulation of Poorly Defined Sub-foveal Choroidal Neovascularization," Ophthalmic Surg., **25**, pp. 195–201.

[5] Weinberger, A. W. A., Knabben, H., Solbach, U., and Wolf, S., 1999, "Indocyanine Green Guided Laser Photocoagulation in Patients With Occult Choroidal Neovascularization," Br. J. Ophthamol., **83**, pp. 168–172.

[6] Maarek, J. I., Holschneider, D. P., and Harimoto, J., 2001, "Fluorescence of Indocyanine Green in Blood: Intensity Dependence on Concentration and Stabilization With Sodium Polyaspartate," J. Photochem. Photobiol., B, **65**, pp. 157–164.

[7] Klein, G. J., Baumgortner, R. H., and Flower, R. W., 1990, "An Image Processing Approach to Characterizing Choroidal Blood Flow," Invest. Ophthalmol. Visual Sci., **31**, pp. 629–637.

[8] Flower, R. W., 1993, "Extraction of Choriocapillaris Hemodynamic Data From ICG Fluorescence Angiograms," Invest. Ophthalmol. Visual Sci., **34**, pp. 2720–2729.

[9] Prunte, C., and Neisel, P., 1988, "Quantification of Choroidal Blood-Flow Parameters Using Indocyanine Green Video-Fluorescence Angiography and Statistical Picture Analysis," Graefe's Arch. Clin. Exp. Ophthalmol., **226**, pp. 55–58.

[10] Ciulla, T. A., Harris, A., Chung, H. S., Danis, R. P., Kagemann, L., Mcnulty, L., Pratt, L. M., and Martin, B. J., 1999, "Color Doppler Imaging Discloses Reduced Ocular Blood Flow Velocities in Nonexudative Age-Related Macular Degeneration," Am. J. Ophthalmol., **128**, pp. 75–80.

[11] Ciulla, T. A., Harris, A., Kagemann, L., Danis, R. P., Pratt, L. M., Chung, H. S., Weinberger, D., and Garzori, H. J., 2002, "Choroidal Perfusion Perturbations in Non-Neovascular Age Related Macular Degeneration," Br. J. Ophthamol., **86**, pp. 209–213.

[12] Paques, M., Garmyn, V., Catier, A., Naoun, K., Vicaut, E., and Gaudric, A., 2001, "Analysis of Retinal and Choroidal Circulation During Central Retinal Vein Occlusion Using Indocyanine Green Videoangiography," Arch. Ophthalmol. (Chicago), **119**, pp. 1781–1787.

[13] Miki, T., Shiraki, K., Kohno, T., Moriwaki, M., and Obana, A., 1996, "Computer Assisted Image Analysis Using the Subtraction Method in Indocyanine Green Angiography," Eur. J. Ophthalmol., **6**, pp. 30–38.

[14] Flower, R. W., 1997, "Physical Optics Concepts Related to Obtaining and Interpreting ICG Angiograms," in *Indocyanine Green: Angiography*, edited by L. Yunnuzzi, Mosby, New York, Chap. 8, pp. 113–114.

[15] Garzozi, H. I., Shoham, N., Chung, H. S., Kagemann, L., and Harris, A., 2001, "Ocular Blood Flow Measurements and Their Importance in Glaucoma and Age-Related Macular Degeneration," IMAJ, **3**, pp. 443–448.

[16] Flower, R. W., and Hochheimer, B. F., 1977, "Quantification of Indicator Dye Concentration in Ocular Blood Vessels," Exp. Eye Res., **25**, pp. 103–111.

[17] Flower, R. W., 1973, "Injection Technique for Indocyanine Green and Sodium Fluorescein Dye Angiography of the Eye," Invest. Ophthalmol., **12**, p. 881.

[18] Flower, R. W., Fryczkowski, A. W., and McLeod, D. S., 1995, "Variability in Choriocapillaris Blood Flow Distribution," Invest. Ophthalmol. Visual Sci., **36**, pp. 1247–1258.

[19] Takasu, I., Shiraga, F., Okanouchi, T., Tsuchida, Y., and Obtsuki, H., 2000, "Evaluation of Leukocyte Dynamics in Choroidal Circulation With Indocyanine Green-Stained Leukocytes," Invest. Ophthalmol. Visual Sci., **41**, pp. 2844–2848.

[20] Michelson, G., Welzenback, J., and Harazny, I. P. J., 2001, "Functional Imaging of the Retinal Microvasculature by Scanning Laser Doppler Flowmetry," Int. Ophthalmol., **23**, pp. 327–335.

[21] Straubhaar, M., Orgul, S., Gugleta, K., Schotzau, A., Erb, C., and Flammer, J., 2000, "Choroidal Laser Doppler Flowmetry in Healthy Subjects," Arch. Ophthalmol. (Chicago), **118**, pp. 211–215.

[22] Durduran, T., Burnett, M. G., Yu, G., Zhou, C., Furuya, D., Yodh, A. G., Detre, J. A., and Greenberg, J. H., 2004, "Spatiotemporal Quantification of Cerebral Blood Flow During Functional Activation in Rat Somatosensory Cortex Using Laser-Speckle Flowmetry," J. Cereb. Blood Flow Metab., **24**, pp. 518–525.

[23] Wimpissinger, B., Resch, H., Berisha, F., Weigert, G., Polak, K., and Schmetterer, L., , "Effects of Isometric Exercise on Subfoveal Choroidal Blood Flow in Smokers and Nonsmokers," Invest. Ophthalmol. Visual Sci., **44**, pp. 4859–4863.

[24] Kimura, S., Yoshioka, T., Shibuya, M., Sakano, T., Tanaka, R., and Matsuyama, S., 2001, "Indocyanine Green Elimination Rate Detects Hepatocellular Dysfunction Early in Septic Shock and Correlates With Survival," Crit. Care Med., **29**, pp. 1159–1163.

[25] Grunwald, J., Hariprasad, S., and DuPont, J., 1998, "Foveal Choroidal Blood Flow in Age-Related Macular Degeneration," Invest. Ophthalmol. Visual Sci., **39**, pp. 385–390.

[26] Spraul, C. W., Lang, G. E., and Grossniklaus, H. E., 1996, "Morphometric Analysis of the Choroid, Bruch's Membrane, and Retinal Pigment Epithelium in Eyes With Age-Related Macular Degeneration," Invest. Ophthalmol. Visual Sci., **37**, pp. 2724–2735.

[27] Kano, K., Kohno, T., Miki, T., and Shiraki, K., 2001, "Rapid Injection of Indocyanine Green Dye for Evaluation of Choroidal Venous Circulation," Jpn. J. Ophthalmol., **45**, pp. 453–462.

[28] Friedman, E., Krupsky, S., Lane, A. M., Oak, S. S., Freidman, E. S., and Egan, K., 1995, "Ocular Blood Flow Velocity in Age-Related Macular Degeneration," Ophthalmology, **102**, pp. 640–646.

[29] Ito, Y. N., Mori, K., Young-Duvall, J., and Yoneya, S., 2001, "Aging Changes of the Choroidal Dye Filling Pattern in Indocyanine Green Angiography of Normal Subjects," Retina, **21**, pp. 237–242.

[30] Flower, R. F., von Kerczek, C., Zhu, L., Earnest, A., Eggleton, C., and Topoleski, L. D. T., 2001, "A Theoretical Investigation of the Role of Choriocapillaris Blood Flow in Treatment of Sub-Foveal Choroidal Neovascularization Associated With Age-Related Macular Degeneration," Am. J. Ophthalmol., **132**, pp. 85–93.